NASA TECHNICAL NOTE

NASA TN D-8056

NASA TN D-8056

A g-LOAD DISPLAY FOR REMOTELY PILOTED VEHICLES AND OTHER AIRCRAFT THAT ARE SUBJECT TO MANEUVERING CONSTRAINTS

James C. Howard

Ames Research Center

Moffett Field, Calif. 94035

NATIONAL AERONAUTICS AND SPACE ADMINISTRATION • WASHINGTON, D. C. • SEPTEMBER 1975

ERRATA

NASA Technical Note D-8056

A g-LOAD DISPLAY FOR REMOTELY PILOTED VEHICLES
AND OTHER AIRCRAFT THAT ARE SUBJECT TO
MANEUVERING CONSTRAINTS

James C. Howard
September 1975

Page 12, last line below the word "that" should be an unnumbered equation to read:

$$\dot{\alpha} = \dot{\beta} = 0$$

Issued March 1976

1 Report No	2 Government Accession No	3 Recipient's Catalog No
NASA TN-8056		

4 Title and Subtitle	5 Report Date
A g-LOAD DISPLAY FOR REMOTELY PILOTED VEHICLES AND OTHER AIRCRAFT THAT ARE SUBJECT TO MANEUVERING CONSTRAINTS	September 1975
	6 Performing Organization Code

7 Author(s)	8 Performing Organization Report No
James C. Howard	A-6032
	10 Work Unit No
	504-09-33-11

9 Performing Organization Name and Address	11 Contract or Grant No
NASA Ames Research Center Moffett Field, Calif. 94035	
	13 Type of Report and Period Covered
12 Sponsoring Agency Name and Address	Technical Note
National Aeronautics and Space Administration Washington, D.C. 20546	14 Sponsoring Agency Code

15 Supplementary Notes

16 Abstract

The absence of kinesthetic cues deprives RPV pilots of essential feedback, particularly during high speed maneuvers. A display has been designed to facilitate pilot control of g loads and to permit an immediate indication of g-load constraint violations. The display embodies all the motion vector components that contribute to maneuvering accelerations. In one mode of operation, the device displays the components of angular velocity as variable length pointers emanating from the center of a circle whose radius is determined by the linear velocity of the vehicle. An alternative mode of operation permits the pilot to select a display in which g loads are presented directly as variable length pointers emanating from the center of a circle whose radius is again determined by the linear velocity of the vehicle Each circle defines a safe region of operation, and penetration of the circumference of the appropriate circle by a pointer implies that the structural design load has been exceeded.

17 Key Words (Suggested by Author(s))	18 Distribution Statement
Display g loads RPV Aircraft display Instrumentation	Unclassified - Unlimited STAR Categories: 06

19 Security Classif (of this report)	20 Security Classif (of this page)	21 No of Pages	22 Price*
Unclassified	Unclassified	17	$3.25

*For sale by the National Technical Information Service, Springfield, Virginia 22161

SYMBOLS

a	total acceleration
$\bar{a}$	total acceleration vector
a_c	critical design acceleration
a_m	maneuvering acceleration
$\bar{a}_m$	maneuvering acceleration vector
$\bar{f}$	resultant inertial and gravitational acceleration vector
g	gravitational constant
$\bar{g}$	gravity vector
g_f	gravitational plus inertial acceleration forces
$\hat{i}, \hat{j}, \hat{k}$	triad of mutually orthogonal unit vectors defining body axes
$\underline{\hat{i}}, \underline{\hat{j}}, \underline{\hat{k}}$	triad of mutually orthogonal unit vectors defining wind axes
m	mass
P, Q, R	effective angular velocity components
p, q, r	angular velocity components relative to body axes
$\bar{p}, \bar{q}, \bar{r}$	angular velocity components relative to wind axes
u, v, w	linear velocity components relative to body axes
$\bar{u}, \bar{v}, \bar{w}$	linear velocity components relative to wind axes
V	resultant linear velocity
$\bar{V}$	resultant linear velocity vector
x, y, z	Cartesian coordinates
α	angle of attack
β	angle of sideslip
η	angle between R and the resultant of R and Q
λ_i	eigenvalues
θ, ϕ	Eulerian angles

$\overline{\Omega}$	combined actual and virtual angular velocity vector
$\overline{\omega}$	angular velocity vector
ω	angular velocity

Subscripts

b	body axes
c	critical design value
e	effective angular velocity
g	virtual angular velocity due to gravity
m	maneuvering
$\overline{q}$	gravitational component in the direction of $\overline{\hat{j}}$
$\overline{r}$	gravitational component in the direction of $\overline{\hat{k}}$
W	wind axes

A g-LOAD DISPLAY FOR REMOTELY PILOTED VEHICLES AND OTHER AIRCRAFT THAT ARE SUBJECT TO MANEUVERING CONSTRAINTS

James C. Howard

Ames Research Center

SUMMARY

The absence of kinesthetic cues deprives RPV pilots of essential feedback, particularly during high speed maneuvers. A display has been designed which presents g-load information in a sufficiently dramatic form to compensate for this deficiency. The display embodies all the motion vector components that contribute to maneuvering accelerations. In one mode of operation, the device displays the angular velocity components as variable length pointers emanating from the center of a circle whose radius is determined by the linear velocity of the vehicle. Inasmuch as this mode of presentation emphasizes the role of the angular velocity vector, while at the same time displaying the influence of the constraint imposed by the linear velocity, it is well suited to the application considered in this report. An alternative mode of operation permits the pilot to select a display in which g loads are presented directly as variable length pointers emanating from the center of a circle whose radius is again determined by the linear velocity of the vehicle. Each circle defines a safe region of operation, and penetration of the circumference of the appropriate circle by a pointer implies that the structural design load has been exceeded.

INTRODUCTION

The overall objective of the remotely piloted vehicle (RPV) program is to develop an aeronautical research tool that is well suited to aerodynamic research; to obtain high angle-of-attack data up to and including post-stall, pre-spin conditions, and to assess advanced control systems under these conditions. In one of its more important applications, the RPV program represents an attempt to reduce the cost and the danger involved in testing high-performance aircraft. The lack of full-scale flight test data for such aircraft is due to the risk involved in testing them. The RPV approach offers a very attractive potential for performing large scale flight testing of hazardous tasks at low risk and relatively low cost (ref. 1). As the RPV program is presently constituted, remotely piloted vehicles are to be flown from fixed-base control centers. In this connection it should be noted that in the absence of inertial motion cues, the RPV pilot is more likely than the pilot of a manned vehicle to exceed the structural capability of his aircraft during high-speed maneuvers.

It is with this aspect of the RPV program that the present report is concerned. The g-load display concept proposed is based on a geometrical inter-

pretation of maneuvering accelerations. Although the maneuvering accelerations can be depicted in vector form, it is more expedient for present purposes to reduce the acceleration to scalar form. The most convenient form is realized by squaring the acceleration vector and reducing the subsequent quadratic form to the canonical form by an orthogonal transformation. The advantage of the canonical representation is that it reveals the geometry of the acceleration in a form which is easily interpreted for display purposes.

It will be seen that gravity can be included without sacrificing the geometrical simplicity of the maneuvering acceleration display. This is accomplished by expressing the gravity vector in terms of a virtual angular velocity vector, which can then be combined with the maneuvering angular velocity vector to give the total inertial and gravitational acceleration.

ANALYSIS

Maneuvering Accelerations

Vehicle accelerations resulting from aerodynamic, thrust, and gravitational forces are given by Coriolis' equation

$$\left(\frac{\partial \overline{V}}{\partial t} + \overline{\omega} \times \overline{V}\right) = \overline{a} \tag{1}$$

The geometrical properties of acceleration become more evident when acceleration is expressed in scalar form. The scalar equivalent of equation (1) is

$$\left(\frac{\partial \overline{V}}{\partial t} + \overline{\omega} \times \overline{V}\right) \cdot \left(\frac{\partial \overline{V}}{\partial t} + \overline{\omega} \times \overline{V}\right) = a^2$$

therefore

$$\left(\frac{\partial \overline{V}}{\partial t}\right)^2 + 2\left(\frac{\partial \overline{V}}{\partial t}\right) \cdot (\overline{\omega} \times \overline{V}) + (\overline{\omega} \times \overline{V})^2 = a^2$$

Moreover, in the absence of accelerations due to $\dot{\alpha}$ and $\dot{\beta}$, $\partial \overline{V}/\partial t$ is parallel to $\overline{V}$, and in this case $\partial \overline{V}/\partial t$ and $\omega \times \overline{V}$ are perpendicular vectors (see appendix). Because of large damping, aircraft response time is short and both $\dot{\alpha}$ and $\dot{\beta}$ rapidly tend to zero (ref. 2). Hence, the assumption of perpendicularity is a valid one and gives rise to conservative estimates of acceleration. This assumption is reflected in the following equations:

$$\left(\frac{\partial \overline{V}}{\partial t}\right) \cdot (\overline{\omega} \times \overline{V}) = 0 \tag{2}$$

and

$$\left(\frac{\partial \overline{V}}{\partial t}\right)^2 + (\overline{\omega} \times \overline{V})^2 = a^2 \tag{3}$$

Now $\partial \overline{V}/\partial t$ is a vector approximately parallel to the flight path, and $\overline{\omega} \times \overline{V}$ is a

vector normal to the flight path. From the point of view of structural integrity, inertia force components normal to the flight path are more important than components parallel to the flight path. This is due to the fact that components normal to the flight path subject the wings and empennage to bending moments that are reacted by the least moments of resistance of these structural units. Hence, the stress-inducing capability of inertia force components normal to the flight path is much greater than that of components parallel to the flight path. For this reason the g loads produced by inertia forces acting parallel to the flight path will be omitted. It should be noted, however, that due to the existence of angles of attack and sideslip, the inertia force components normal to the flight path are not always normal to the wing and stabilizer plan forms. However, the errors introduced by assuming normality are on the conservative side.

A maneuvering acceleration resulting from changes in aircraft attitude is defined as follows:

$$(\bar{\omega} \times \bar{V}) = \bar{a}_m \tag{4}$$

Relative to an orthogonal Cartesian coordinate system, the vector $\bar{a}_m$ assumes the following form:

$$\bar{a}_m = [(qw - rv)\hat{i} + (ru - pw)\hat{j} + (pv - qu)\hat{k}] \tag{5}$$

where $\hat{i}$, $\hat{j}$ and $\hat{k}$ are a triad of mutually orthogonal unit vectors.

As already indicated, it is more expedient for display purposes to reduce the acceleration from the vector form of equation (4) to the following scalar forms:

$$(\bar{\omega} \times \bar{V}) \cdot (\bar{\omega} \times \bar{V}) = a_m^2 \tag{6}$$

therefore

$$a_m^2 = [V^2 \omega^2 - (\bar{V} \cdot \bar{\omega})^2] \tag{7}$$

In terms of the linear and angular velocity components, equation (7) may be expanded as follows:

$$a_m^2 = [(v^2 + w^2)p^2 + (u^2 + w^2)q^2 + (u^2 + v^2)r^2 - 2(uvpq + uwpr + vwqr)] \tag{8}$$

Equation (8) reveals that a_m^2 is a quadratic form. By a suitable transformation of axes, a quadratic form can be reduced to the canonical form

$$a_m^2 = (\lambda_1 \bar{p}^2 + \lambda_2 \bar{q}^2 + \lambda_3 \bar{r}^2)$$

where $\bar{p}$, $\bar{q}$, $\bar{r}$ are the components of the angular velocity vector in the new system of axes and λ_i are the corresponding eigenvalues (ref. 3).

In the present case, the required canonical form can be obtained by choosing a system of axes such that the angular velocity component $\bar{p}$ coincides with the linear velocity vector $\bar{V}$. Although the axes for the specification of

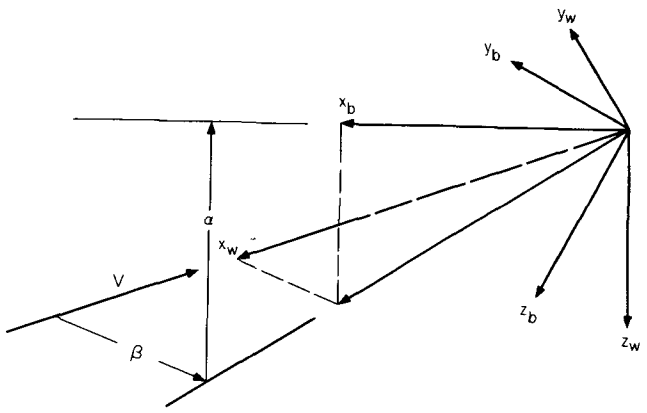

Figure 1. — Systems of reference axes, including body and wind.

the components $\overline{q}$ and $\overline{r}$ may be chosen arbitrarily, provided they are orthogonal to each other and to the linear velocity vector $\overline{V}$, the arrangement shown in figure 1 has been adopted. Thus, relative to the new reference frame, the eigenvalues are

$$\lambda_1 = 0 \ , \quad \lambda_2 = V^2 \ , \quad \lambda_3 = V^2$$

and a_m^2 assumes the form

$$(V^2 \overline{q}^2 + V^2 \overline{r}^2) = a_m^2 \qquad (9)$$

which represents a circular cylinder.

It follows from equation (9) that, for an allowable acceleration a_c, the angular velocity vector $\overline{\omega}$ is bounded by the surface of a circular cylinder of radius a_c/V, having for its axis the linear velocity vector $\overline{V}$.

Gravity Components

In order to retain the geometrical simplicity of the maneuvering g-load display, the gravity components may be treated as virtual angular rates. This results in adjustments to the pointer length to reflect the instantaneous magnitudes of the gravity components, while leaving the circle unchanged. For this purpose, it is necessary to refer the gravity components to a set of wind axes. The axes are chosen such that the x axis coincides with the wind vector, and the y and z axes assume the orientations shown in figure 1.

Wind axes are related to body axes as follows:

$$\begin{pmatrix} x \\ y \\ z \end{pmatrix}_W = \begin{pmatrix} \cos\alpha \cos\beta & \sin\beta & \sin\alpha \cos\beta \\ -\cos\alpha \sin\beta & \cos\beta & -\sin\alpha \sin\beta \\ -\sin\alpha & 0 & \cos\alpha \end{pmatrix} \begin{pmatrix} x \\ y \\ z \end{pmatrix}_B$$

where

$$\begin{pmatrix} x \\ y \\ z \end{pmatrix}_W \quad \text{and} \quad \begin{pmatrix} x \\ y \\ z \end{pmatrix}_B$$

are column vectors of coordinates in the wind and body axes respectively, and

$$\beta = \sin^{-1}(v/V) \; ; \qquad \alpha = \tan^{-1}(w/u)$$

The gravity vector has body axis components,

$$\bar{g} = g(-\sin\theta\hat{i} + \cos\theta \sin\phi\hat{j} + \cos\theta \cos\phi\hat{k})$$

where θ and ϕ are Eulerian angles relating the body axes to a set of earth fixed reference axes (ref. 2). Hence, the components of gravity in the direction of the wind axes of interest are:

$$g_{\bar{q}} = g(\sin\theta \cos\alpha \sin\beta + \cos\theta \sin\phi \cos\beta - \cos\theta \cos\phi \sin\alpha \sin\beta)$$

and

$$g_{\bar{r}} = g(\sin\theta \sin\alpha + \cos\theta \cos\phi \cos\alpha)$$

Moreover,

$$\bar{q} = (-p \cos\alpha \sin\beta + q \cos\beta - r \sin\alpha \sin\beta)$$

and

$$\bar{r} = (-p \sin\alpha + r \cos\alpha)$$

The g-load display is required to indicate the instantaneous value of the inertial and gravitational forces to which the aircraft is exposed. The sum of these forces is given by

$$-m\bar{a}_m + m\bar{g} = -m(\bar{a}_m - \bar{g}) = m\bar{f}$$

therefore

$$\bar{f} = -(\bar{a}_m - \bar{g}) = -(\bar{\omega} \times \bar{V} - \bar{g})$$

or

$$\bar{f} = \left[\bar{g} - V\left(\bar{r}\hat{j} - \bar{q}\hat{k}\right)\right]$$

where $\hat{i}$, $\hat{j}$, and $\hat{k}$ are a triad of mutually orthogonal unit vectors specifying the directions of the wind axis. Therefore,

$$\bar{f} = \Big\{ [g(\sin\theta \cos\alpha \sin\beta + \cos\theta \sin\phi \cos\beta - \cos\theta \cos\phi \sin\alpha \sin\beta)$$
$$- V(-p \sin\alpha + r \cos\alpha)]\hat{j} + [g(\sin\theta \sin\alpha + \cos\theta \cos\phi \cos\alpha)$$
$$+ V(-p \cos\alpha \sin\beta + q \cos\beta - r \sin\alpha \sin\beta)]\hat{k} \Big\}$$

This equation may be rewritten as follows:

$$\bar{f} = V\left\{\left[\frac{g}{V}(\sin\theta\cos\alpha\sin\beta + \cos\theta\sin\phi\cos\beta - \cos\theta\cos\phi\sin\alpha\sin\beta)\right.\right.$$

$$\left. - (-p\sin\alpha + r\cos\alpha)\right]\hat{j} + \left[\frac{g}{V}(\sin\theta\sin\alpha + \cos\theta\cos\phi\cos\alpha)\right.$$

$$\left.\left. + (-p\cos\alpha\sin\beta + q\cos\beta - r\sin\alpha\sin\beta)\right]\hat{k}\right\}$$

The combined inertial and gravitational accelerations may now be expressed in the alternative form

$$\bar{f} = -\bar{\Omega}\times\bar{V}$$

where

$$\bar{\Omega} = P\hat{i} + Q\hat{j} + R\hat{k}$$

Hence,

$$m\bar{f} = mV\left(Q\hat{k} - R\hat{j}\right) \tag{10}$$

therefore

$$Q = \left[(-p\cos\alpha\sin\beta + q\cos\beta - r\sin\alpha\sin\beta)\right.$$

$$\left. + \frac{g}{V}(\sin\theta\sin\alpha + \cos\theta\cos\phi\cos\alpha)\right] \tag{11}$$

or

$$Q = (\bar{q} + \bar{q}_g)$$

where

$$\bar{q} = (-p\cos\alpha\sin\beta + q\cos\beta - r\sin\alpha\sin\beta)$$

and

$$\bar{q}_g = \frac{g}{V}(\sin\theta\sin\alpha + \cos\theta\cos\phi\cos\alpha)$$

The term $\bar{q}_g$ is the virtual angular velocity relative to the $\hat{j}$ wind axes corresponding to the gravitational component of acceleration.

Likewise,

$$R = \left[(-p \sin\alpha + r \cos\alpha) - \frac{g}{V}(\sin\theta \cos\alpha \sin\beta + \cos\theta \sin\phi \cos\beta - \cos\theta \cos\phi \sin\alpha \sin\beta)\right] \tag{12}$$

or

$$R = (\bar{r} + \bar{r}_g)$$

where

$$\bar{r} = (-p \sin\alpha + r \cos\alpha)$$

and

$$\bar{r}_g = -\frac{g}{V}(\sin\theta \cos\alpha \sin\beta + \cos\theta \sin\phi \cos\beta - \cos\theta \cos\phi \sin\alpha \sin\beta)$$

where $\bar{r}_g$ is the virtual angular velocity in the direction of the $\hat{k}$ axis, corresponding to the gravitational component of acceleration.

Therefore, the motion vector components to be utilized for display purposes are Q, R, and f, which are related as follows:

$$(V^2Q^2 + V^2R^2) = f^2 \tag{13}$$

The effective angular velocity, which now includes the virtual components due to gravity, is

$$(Q^2 + R^2) = \omega_e{}^2 = f^2/V^2 \tag{14}$$

and is inclined at an angle η to the $\hat{j}$ axis, where

$$\eta = \tan^{-1}(R/Q) \tag{15}$$

Equation (13) has the same form as equation (9). It follows that for an allowable acceleration a_c, the effective angular velocity vector $\bar{\omega}_\epsilon$ is still bounded by the surface of a circular cylinder of radius a_c/V.

The critical design loads in the positive and negative directions of the unit vector $\hat{k}$ are asymmetrical and different from the symmetrical design load in the direction of the unit vector $\hat{j}$. The display format for the motion vector components given by equation (14) is shown in figure 2(a), where the different critical design loads

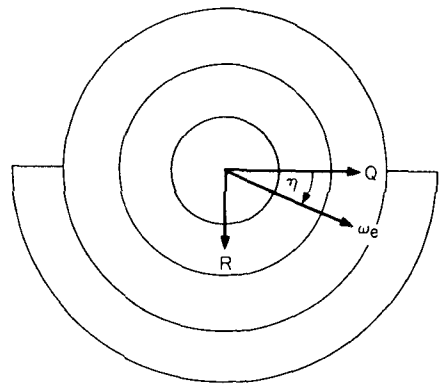

(a) Angular velocity.

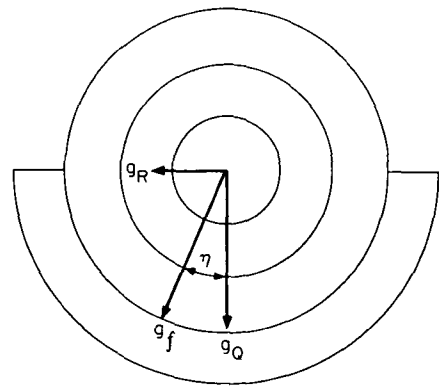

(b) Acceleration.

Figure 2. — Display of motion vector components.

are represented by different circles. However, the use of more than one circle can be avoided, if desired, by using appropriate scaling factors for the different pointers.

It should be noted that figure 2(a) displays the motion vector components that give rise to the maneuvering g forces. This has been done to facilitate pilot control of the motion components that produce these forces. Equation (10) gives the actual force components produced. The display format which gives the directions of these components can be obtained by rotating figure 2(a) through a positive angle of 90°, as shown in figure 2(b).

Implementation

In practical applications, the g-load display can be mechanized to show the angular-velocity components as variable-length pointers emanating from the center of a circle whose radius is determined by the linear velocity of the aircraft. Inasmuch as this mode of presentation emphasizes the role of the angular velocity vector, while at the same time displaying the influence of the constraint imposed by the linear velocity, it is well suited to the application considered in this report.

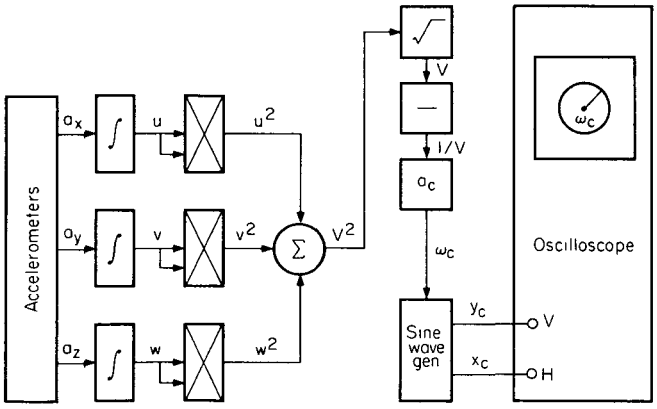

Figure 3. — Apparatus for processing accelerometer data.

Figure 3 shows a diagram of the apparatus required to generate the constraint circle. Three body-mounted accelerometers provide three output signals whose values are equal to the three linear acceleration components a_x, a_y, a_z of the aircraft relative to body axes. Also provided is an input signal a_c which is indicative of the maximum design load of the aircraft in which the apparatus is placed. The three acceleration components are then passed through three integrators which yield the three velocity components u, v, and w. The velocity components are squared and summed to obtain V^2. The remaining circuitry extracts the square root of V^2, determines its reciprocal, and formulates the signal $\omega_c = a_c/V$ which is indicative of the instantaneous critical angular velocity. This is the angular velocity which would produce g loads sufficient to cause structural failure at the given velocity. As seen in figure 3, the signal is then passed through a sine wave generator to an oscilloscope to produce the circle shown. Before proceeding to generate the instantaneous values of the angular-velocity components Q and R in accordance with equations (11) and (12), it is necessary to generate the angles α and β, and to measure the components p, q, r and the Euler angles θ and ϕ.

The velocity components generated by the apparatus shown in figure 3 may be used to determine the angles of attack and sideslip and their trigonometric functions as shown in figure 4.

The three body-mounted rate gyros shown in figure 5(a) are required to measure the instantaneous values p, q, and r of the vehicle's angular velocity relative to body axes. The two position-gyros shown in figure 5(b) are used to measure the Eulerian angles θ and ϕ.

This completes the apparatus needed to measure and generate the information required to formulate the components Q and R in accordance with equations (11) and (12). The output from the pieces of apparatus described can be combined by the use of multipliers and summers, to yield the components of the inertial and gravitational forces acting on an aircraft during maneuvers.

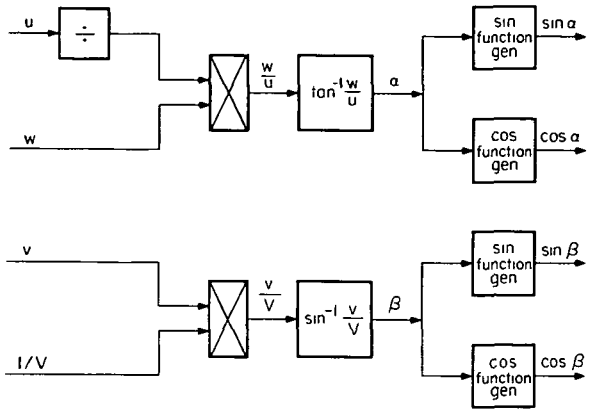

Figure 4. — Apparatus for generating angles of attack and sideslip and their trigonometric functions.

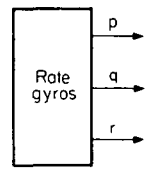

(a) Measuring body rates.

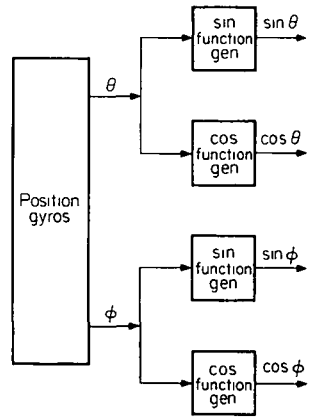

(b) Measuring Euler angles and generating their trigonometric functions.

Figure 5. — Apparatus for measuring rate and attitude.

CONCLUSIONS

A display has been designed to facilitate control of g loads during remotely piloted vehicle maneuvers and to provide an immediate indication of g-load constraint violations. It is shown that for an allowable acceleration a_c, the angular velocity vector $\overline{\omega}$ is bounded by the surface of a circular cylinder of radius a_c/V, which has for its axis the linear velocity vector $\overline{V}$. For a specified value of a_c, the cylinder expands or contracts as the aircraft velocity varies, thus indicating to the pilot the linear and angular velocities permitted for a given acceleration constraint. In practical applications it is adequate to generate a circular cross section of a cylinder. When this form of display is used to facilitate pilot control of g loads, pointers move in a circle of radius a_c/V and assume lengths indicative of the acceleration-producing components of

angular velocity. An alternative mode of operation permits the pilot to select a display in which g loads are presented directly as variable length pointers emanating from the center of a circle whose radius is again determined by the linear velocity of the vehicle.

Ames Research Center
National Aeronautics and Space Administration
Moffett Field, Calif., 94035, June 3, 1975

APPENDIX A

CONDITIONS FOR THE PARALLELISM OF THE VECTORS $\overline{V}$ AND $\partial\overline{V}/\partial t$

To determine the conditions for the parallelism of the vectors $\overline{V}$ and $\partial\overline{V}/\partial t$, it is first necessary to show that

$$\frac{\partial V}{\partial t} = (\dot{u}\hat{i} + \dot{v}\hat{j} + \dot{w}\hat{k}) \tag{A1}$$

Proof:

Let $$u = (\overline{V} \cdot i)$$

therefore

$$\dot{u} = \frac{du}{dt} = \frac{d}{dt}(\overline{V} \cdot i)$$

$$\dot{u} = \left(\frac{d\overline{V}}{dt} \cdot \hat{i} + \overline{V} \cdot \frac{d\hat{i}}{dt}\right)$$

that is

$$\dot{u} = \left[\left(\frac{\partial\overline{V}}{\partial t} + \overline{\omega} \times \overline{V}\right) \cdot \hat{i} + \overline{V} \cdot \frac{d\hat{i}}{dt}\right] \tag{A2}$$

but

$$\frac{d\hat{i}}{dt} = \left(\frac{\partial\hat{i}}{\partial t} + \overline{\omega} \times \hat{i}\right) = \overline{\omega} \times \hat{i} \tag{A3}$$

Substitution from equation (A3) in equation (A2) gives

$$\dot{u} = \left[\frac{\partial\overline{V}}{\partial t} \cdot \hat{i} + (\overline{\omega} \times \overline{V}) \cdot \hat{i} + \overline{V} \cdot (\overline{\omega} \times \hat{i})\right]$$

This equation may be rewritten as follows:

$$\dot{u} = \left[\frac{\partial\overline{V}}{\partial t} \cdot \hat{i} - (\overline{V} \times \overline{\omega}) \cdot \hat{i} + (\overline{V} \times \overline{\omega}) \cdot \hat{i}\right]$$

therefore

$$\dot{u} = \left(\frac{\partial\overline{V}}{\partial t} \cdot \hat{i}\right)$$

likewise

$$\dot{v} = \left(\frac{\partial \overline{V}}{\partial t} \cdot \hat{j}\right)$$

and

$$\dot{w} = \left(\frac{\partial \overline{V}}{\partial t} \cdot \hat{k}\right)$$

therefore

$$(\dot{u}\hat{i} + \dot{v}\hat{j} + \dot{w}\hat{k}) = \frac{\partial \overline{V}}{\partial t} \cdot (\hat{i}\hat{i} + \hat{j}\hat{j} + \hat{k}\hat{k})$$

or

$$(\dot{u}\hat{i} + \dot{v}\hat{j} + \dot{w}\hat{k}) = \frac{\partial \overline{V}}{\partial t} \cdot \overline{\Phi} = \frac{\partial \overline{V}}{\partial t} \tag{A4}$$

where $\overline{\Phi}$ is the idemfactor.

The parallelism conditions must ensure that $\partial \overline{V}/\partial t$ has no component perpendicular to $\overline{V}$. Hence, it is sufficient to show that, subject to the established conditions

$$\overline{V} \times \frac{\partial \overline{V}}{\partial t} = 0 \tag{A5}$$

This equation may be rewritten in component form as follows:

$$\left(\overline{V} \times \frac{\partial \overline{V}}{\partial t}\right) = \left[(v\dot{w} - w\dot{v})\hat{i} + (w\dot{u} - u\dot{w})\hat{j} + (u\dot{v} - v\dot{u})\hat{k}\right] \tag{A6}$$

Moreover

$$u = V \cos\alpha \cos\beta$$

$$v = V \sin\beta$$

$$w = V \sin\alpha \cos\beta$$

Substitution of these values in equation (A6) yields the following conditions for the parallelism of the vectors $\overline{V}$ and $\partial \overline{V}/\partial t$

$$[(\cos\alpha \sin\beta \cos\beta)\dot{\alpha} - (\sin\alpha)\dot{\beta}] = 0$$

$$(\cos^2\beta)\dot{\alpha} = 0$$

$$(\sin\alpha \sin\beta \cos\beta)\dot{\alpha} + (\cos\alpha)\dot{\beta} = 0$$

Consequently, the condition of parallelism will be satisfied, provided that

REFERENCES

1. Howard, James C.: Display Requirements for the Final Approach and Landing Phase of an RPV Mission. NASA TM X-62,346, April 1974.

2. Etkin, Bernard: Dynamics of Atmospheric Flight. John Wiley & Sons, Inc., 1959.

3. Goldstein, Herbert: Classical Mechanics. Addison-Wesley Publishing Company, Inc., 1957.

"The aeronautical and space activities of the United States shall be conducted so as to contribute . . to the expansion of human knowledge of phenomena in the atmosphere and space The Administration shall provide for the widest practicable and appropriate dissemination of information concerning its activities and the results thereof"

—NATIONAL AERONAUTICS AND SPACE ACT OF 1958

NASA SCIENTIFIC AND TECHNICAL PUBLICATIONS

TECHNICAL REPORTS: Scientific and technical information considered important, complete, and a lasting contribution to existing knowledge

TECHNICAL NOTES Information less broad in scope but nevertheless of importance as a contribution to existing knowledge

TECHNICAL MEMORANDUMS Information receiving limited distribution because of preliminary data, security classification, or other reasons. Also includes conference proceedings with either limited or unlimited distribution.

CONTRACTOR REPORTS Scientific and technical information generated under a NASA contract or grant and considered an important contribution to existing knowledge

TECHNICAL TRANSLATIONS Information published in a foreign language considered to merit NASA distribution in English

SPECIAL PUBLICATIONS Information derived from or of value to NASA activities. Publications include final reports of major projects, monographs, data compilations, handbooks, sourcebooks, and special bibliographies.

TECHNOLOGY UTILIZATION PUBLICATIONS Information on technology used by NASA that may be of particular interest in commercial and other non-aerospace applications Publications include Tech Briefs, Technology Utilization Reports and Technology Surveys.

Details on the availability of these publications may be obtained from:

SCIENTIFIC AND TECHNICAL INFORMATION OFFICE

NATIONAL AERONAUTICS AND SPACE ADMINISTRATION

Washington, D.C. 20546